0026-895X/04/6605-1093–1102$20.00
MOLECULAR PHARMACOLOGY
Vol. 66, No. 5
1065/1178041

Mol Pharmacol 66:1093–1102, 2004
Printed in U.S.A.

A Common Antitussive Drug, Clobutinol, Precipitates the Long QT Syndrome 2

Chloé Bellocq, Ronald Wilders, Jean-Jacques Schott, Bénédicte Louérat-Oriou, Pierre Boisseau, Hervé Le Marec, Denis Escande, and Isabelle Baró

l'institut du thorax, Institut National de la Sante et de la Recherche Medicale U533, Nantes, France (C.B., J.J.S., B.L.O., H.L.M., D.E., I.B.); Department of Physiology, Academic Medical Center, University of Amsterdam, Amsterdam, the Netherlands (R.W.); Laboratoire de Génétique Moléculaire, CHU de Nantes, Nantes, France (P.B.); and Clinique Cardiologique et des Maladies Vasculaires, Centres d'Investigation Clinique Institut National de la Sante et de la Recherche Medicale de Nantes, Nantes, France (H.L.M.)

Received April 2, 2004; accepted July 27, 2004

ABSTRACT

QT prolongation, a classic risk factor for arrhythmias, can result from a mutation in one of the genes governing cardiac repolarization and also can result from the intake of a medication acting as blocker of the cardiac K^+ channel human *ether-a-go-go*-related gene (HERG). Here, we identified the arrhythmogenic potential of a nonopioid antitussive drug, clobutinol. The deleterious effects of clobutinol were suspected when a young boy, with a diagnosis of congenital long QT syndrome, experienced arrhythmias while being treated with this drug. Using the patch-clamp technique, we showed that clobutinol dose-dependently inhibited the HERG K^+ current with a half-maximum block concentration of 2.9 μM. In the proband, we identified a novel A561P HERG mutation. Two others long QT mutations (A561V and A561T) had been reported previously at the same position. None of the three mutants led to a sizeable current in heterologous expression system. When coexpressed with wild-type (WT) HERG channels, the three Ala561 mutants reduced the trafficking of WT and mutant heteromeric channels, resulting in decreased K^+ current amplitude (dominant-negative effects). In addition, A561P but not A561V and A561T mutants induced a ≈ -11 mV shift of the current activation curve and accelerated deactivation, thereby partially counteracting the dominant-negative effects. A561P mutation and clobutinol effects on the human ventricular action potential characteristics were simulated using the Priebe-Beuckelmann model. Our work shows that clobutinol has limited effects on WT action potential but should be classified as a "drug to be avoided by congenital long QT patients" rather than as a "drug with risk of torsades de pointes".

QT prolongation is a risk factor in a number of cardiovascular and noncardiovascular diseases. Among these, the congenital form of the long QT syndrome (LQT) associates prolonged rate-corrected QT interval (QTc) with recurrent syncope and sudden cardiac death resulting from torsades de pointes tachyarrhythmias. The long QT syndrome may also result from the effects of numerous chemically unrelated medications (acquired LQT) in patients with pre-existing normal QT or in patients carrying a long QT gene mutation. At the cellular level, prolongation of the QT interval reflects lengthening of the ventricular action potential (AP). In the human heart, a key repolarizing potassium current is the rapidly activating component of the delayed rectifier I_{Kr} (Sanguinetti and Jurkiewicz, 1990). Its activation initiates repolarization and terminates the plateau phase of the cardiac AP concomitantly to the T wave on the ECG. I_{Kr} is related to pore-forming channel proteins encoded by the human *ether-a-go-go*-related gene (*HERG*) (Curran et al., 1995; Sanguinetti et al., 1995). Mutations in *HERG* account for chromosome 7-linked inherited long QT syndrome 2 (LQT2) (Keating, 1995; Sanguinetti et al., 1996). Finally, the vast majority of drugs that produce the acquired LQT are blockers of HERG channels (Roden et al., 1996).

In the present work, we have identified the arrhythmogenic potential of a common drug, clobutinol, a centrally acting nonopioid antitussive drug widely used in Europe as

This work was supported by the Fondation de France and INSERM. C.B. is financially supported by INSERM/Pays-de-Loire. I.B. is recipient of a tenure position supported by the Centre National de la Recherche Scientifique.
Article, publication date, and citation information can be found at http://molpharm.aspetjournals.org.
doi:10.1124/mol.104.001065.

ABBREVIATIONS: LQT, long QT syndrome; AP, action potential; HERG, human *ether-a-go-go*-related gene; I_{Kr}, rapidly activating component of the cardiac delayed rectifier K^+ current; QTc, rate-corrected QT interval; WT, wild type; LQT2, long QT syndrome 2; PEI, polyethylenimine; APD, action potential duration; EAD, early after-depolarization; ΔAPD_{90}, change in action potential duration at 90% repolarization; E-4031, 1-[2-(6-methyl-2-pyridyl)ethyl]-4-methylsulfonylaminobenzoyl)piperidine.

treatment for dry cough of infectious origin. The deleterious effects of the molecule were suspected when a young boy, with a diagnosis of LQT2, experienced syncopes and arrhythmias while being treated with clobutinol. We have evaluated the inhibitory potency of clobutinol on wild-type HERG current. In the proband, we identified a novel LQT2 mutation (A561P), which we functionally characterized in recombinant expression system. It is interesting to note that two others mutations (A561V and A561T) at the same position were reported previously (Curran et al., 1995; Dausse et al., 1996) in patients with congenital LQT2. We thus examined and compared the mechanism for HERG channel dysfunction in each of these three A561 mutations. Our work shows that a common drug not identified previously as a QT-prolonging drug can precipitate the LQT2 syndrome.

Materials and Methods

Clinical Studies. The proband, an 11-year-old boy, received a diagnosis of a long QT duration in 1997. In 1999, he developed first symptoms in relation to torsades de pointes upon clobutinol treatment. A familial investigation was initiated. All family members enrolled gave written informed consent. Signature was given by parents in the case of children younger than 18 years. The protocol was approved by the local Committee for the Protection of Human Subjects in Biomedical Research of Nantes University, Nantes, France. Participants were evaluated by history, review of medical records, and 12-lead electrocardiogram. Correction of the duration of the QT interval as a function of cycle length was performed using both Bazett's and Fridericia's formulae ($QTc_{Bazett} = QT/2\sqrt{RR}$ and $QTc_{Fridericia} = QT/3\sqrt{RR}$, with RR expressed in seconds).

Mutation Analysis. Genomic DNA was prepared from peripheral blood lymphocytes by standard methods. Mutation analysis was conducted by direct sequencing of the gene using an ABI 377 automated sequencer (Applied Biosystems, Foster City, CA). Polymerase chain reactions for each of the amplicons representing the entire coding sequence and splicing sites of *KCNH2* as well as *KCNQ1*, *KNCE1,* and *SCN5A* genes were performed as described previously (Wang et al., 1995; Splawski et al., 1998).

Cell Culture and Transfection. African green monkey kidney cells (COS-7) were obtained from the American Type Culture Collection (Manassas, VA). Cells were cultured at 37°C in a 5% CO_2 humidified incubator in Dulbecco's modified Eagle's medium supplemented with 10% fetal calf serum, 2 mM L-glutamine, and antibiotics (100 IU/ml penicillin and 100 μg/ml streptomycin) (all from Invitrogen, Carlsbad, CA). Human wild-type HERG cDNA was subcloned into the mammalian expression vector pBK under the control of the cytomegalovirus promoter/enhancer (Stratagene, La Jolla, CA). A561P, A561T, or A561V mutations were introduced using standard molecular techniques. Cells were transfected using the intranuclear microinjection technique or using polyethylenimine (PEI) as a transfection reagent. A green fluorescence protein plasmid (pEGFP; BD Biosciences Clontech, Palo Alto, CA) was used as an inert plasmid to ensure a constant plasmid concentration and also to permit cell detection. The microinjection protocol using the ECET microinjector 5246 system (Eppendorf, Hamburg, Germany) has been described previously by Mohammad-Panah et al. (1998). Plasmids (3 μg/ml pBK-CMV-WT or mutated HERG plus 3 μg/ml pEGFP for homomeric channels, and 3 μg/ml pBK-CMV-WT HERG plus 3 μg/ml pBK-CMV–mutated HERG for heteromeric channels) were diluted in a buffer containing 40 mM NaCl, 50 mM HEPES, and 50 mM NaOH, pH 7.4, and supplemented with 0.5% fluorescein isothiocyanate-dextran (150 kDa). Otherwise, cells were transfected when the culture reached 60 to 80% confluence with plasmids complexed with PEI as reported previously (Pollard et al., 1998) with 2 μg of plasmids per milliliter of culture medium. In patch-clamp experiments, we used 20% pBK-CMV-WT or mutated HERG plus 80% pEGFP for homomeric channels and 20% pBK-CMV-WT HERG plus 20% pBK-CMV–mutated HERG and 60% pEGFP for heteromeric channels. For immunolocalization experiments, we used 100% pBK-CMV-WT or mutated HERG for homomeric channels and 50% pBK-CMV-WT HERG plus 50% pBK-CMV–mutated HERG for heteromeric channels.

Patch-Clamp Recordings. Twelve to twenty-four hours after transfection, K^+ currents from HERG-transfected COS-7 cells were recorded at 35°C using the whole-cell configuration of the patch-clamp technique. Cells were placed on the stage of an inverted microscope and continuously superfused with Tyrode's solution. During the current measurements, a microperfusion system allowed local application and rapid change of the different extracellular solutions used to specifically record the K^+ currents. Patch pipettes with a tip resistance of 2.5 to 5 MΩ were electrically connected to a patch-clamp amplifier (Axopatch 200A; Axon Instruments Inc., Union City, CA). Stimulation, data recording, and analysis were performed through an A/D converter (Tecmar TM100 Labmaster; Scientific Solutions, Mentor, OH) using Acquis1 software (Bio-Logic, Claix, France). Wild-type (WT) and mutant HERG currents were measured using the following voltage protocol. The membrane potential was clamped at a holding potential of −90 mV, and every 3 s, a voltage prepulse to +10 mV was applied for 500 ms followed by the test pulse to −70 mV for another 500 ms. The deactivating K^+ current (or tail current) was measured during polarization to −70 mV and normalized for each cell using the cell capacitance. To evaluate the current activation, the prepulse voltage varied from −100 to +60 mV for 500 ms. To evaluate the deactivation kinetics, the voltage test pulse varied from −70 to −40 mV. Recorded human subendocardiac action potential acquired at 1000-ms pacing length was also used to clamp the cells.

Immunolocalization Experiments. Cells were plated 12 h after transfection on coverslips, left for 48 h in the incubator to allow protein expression, and then fixed in 4% phosphonoformatic acid, permeabilized in 0.1% Triton X-100, and incubated overnight at 4°C with a rabbit anti-erg antibody (1:1000; Alomone Labs, Jerusalem, Israel) in 1% bovine serum albumin. Cells were rinsed in phosphate-buffered saline and incubated for 1 h at room temperature with a fluorescein isothiocyanate-conjugated goat anti-rabbit antibody (1:200; Sigma-Aldrich, St. Louis, MO). Cells were mounted between slips and coverslips and placed on the stage of an inverted TCS NT confocal microscope (Leica, Wetzlar, Germany). Cells were observed using a ×63 oil objective.

Solutions and Drugs. Tyrode's solution used for patch-clamp experiments contained 145 mM NaCl, 4 mM KCl, 1 mM $MgCl_2$, 1 mM $CaCl_2$, 5 mM HEPES, and 5 mM glucose, pH 7.4. The standard extracellular solution to record K^+ current contained 145 mM sodium gluconate, 4 mM potassium gluconate, 7 mM hemi-calcium gluconate (free Ca^{2+}: 1), 4 mM hemi-magnesium gluconate (free-Mg^{2+}: 1), 5 mM HEPES, 5 mM glucose, and 20 mM mannitol, pH 7.4. Patch-clamp pipettes contained 145 mM potassium gluconate, 2 mM K_2ATP, 2 mM hemi-magnesium gluconate (free-Mg^{2+}: 0.1), 5 mM HEPES, and 2 mM EGTA, pH 7.2. Free activities were calculated using a software designed by G. L. Smith (University of Glasgow, Glasgow, UK). Clobutinol (SILOMAT 20 mg/2 ml solution; Boehringer Ingelheim GmbH, Ingelheim, Germany) was diluted in extracellular solution as a 10^{-4} M stock solution. The test solutions were prepared by further successive dilutions. E-4031 was prepared as a 10^{-3} M stock solution with distilled water.

Computer Modeling. Functional effects of the HERG mutations were tested by computer simulations using the Priebe-Beuckelmann human ventricular cell model (Priebe and Beuckelmann, 1998). The experimentally observed ≈70% reduction in HERG tail current density was implemented by a 70% decrease in the fully activated conductance of I_{Kr}. The experimentally observed −11 mV shift in voltage dependence of WT + A561P HERG current activation was incorporated by a −11 mV shift in the I_{Kr} steady-state activation

curve, whereas the ≈30% decrease in the fast and slow time constants of HERG channel deactivation were implemented by a 30% decrease in the corresponding I_{Kr} time constant. Action potentials were elicited by repetitive stimulation with a 2-ms, ≈20% suprathreshold stimulus current.

The Priebe-Beuckelmann model produces an action potential that is typical for an epicardial cell. To obtain endocardial and M cell models, we reduced the current densities of the transient outward current (I_{to}), the slow component of the delayed rectifier current (I_{Ks}), and the inward rectifier current (I_{K1}) in the Priebe-Beuckelmann model by 75, 8, and 11%, and by 13, 54, and 26%, respectively (Conrath et al., 2004), from canine and human data (Liu et al., 1993; Liu and Antzelevitch, 1995; Näbauer et al., 1996).

To measure restitution of action potential duration (APD restitution) in the single human ventricular cell model, we used an S1–S2 stimulus protocol (Qu et al., 1999). After a period of pacing at a basic S1–S1 pacing interval of 1000 ms, S2 was applied after a variable S1–S2 interval. The strengths of the 2-ms S1 and S2 stimuli were fixed at 2.5 times threshold, and APD was defined using a threshold voltage of −77.2 mV, which is near the voltage at which the action potential is 90% repolarized.

Models were coded using Compaq Visual Fortran 6.6 and run on a 3-GHz Intel Pentium 4 processor workstation, applying a Euler-type integration scheme with a 5-μs step. All simulations were run for a sufficiently long time to reach steady-state behavior.

Statistics. All data are presented as mean ± S.E.M. Statistical significance of the observed effects was assessed by means of the Student's t test, Mann-Whitney rank sum test, or two-way analysis of variance when appropriate. A value of $p < 0.05$ was considered significant.

Results

Clinical Characteristics. The proband, a boy born in 1992, received a diagnosis for a tetralogy of Fallot and had surgery several years before the drug-induced arrhythmia. His ECG follow-up is illustrated in Fig. 1A, a to d. Lengthening of the QT interval (QTc_{Bazett} = 628 ms and $QTc_{Fredericia}$ = 597 ms) was initially detected in 1997 in the absence of associated symptoms (Fig. 1Aa). In 1999, he experienced for the first time syncope and torsades de pointes arrhythmias during treatment with clobutinol, a common antitussive drug (Fig. 1Ab). The baseline serum K^+ level indicated a moderate hypokalemia to 3.5 mM before any treatment (February 5, 1999). However, the arrhythmic episodes did not cease under potassium, magnesium, or β-blocker therapy, even when the serum potassium was normalized to 4.1 mM. Torsades de pointes only ceased when the heart was paced. After clobutinol treatment was discontinued, the QTc interval progressively decreased to pretreatment values with a time course comparable with clobutinol half-life (23–32 h) (Zimmer et al., 1977) (Fig. 1Ac). The kidney function was considered to be normal from urea and creatinine levels [February 5, 1999: 1.8 mM (blood urea nitrogen, 5 mg/dl) and 44 mg/dl, respectively]. After 1999, the proband had no further arrhythmia or symptoms, although he has retained a long QTc interval (Fig. 1Ad). Together, these data correlate the clobutinol intake to the torsades de pointes episodes. Repolarization abnormalities were also detected in his asymptomatic father (Fig. 1B) and in his elder brother (Fig. 1C). Neither the brother nor the father has had a history of cardiac surgery. The other relatives, including his mother (Fig. 1D), presented normal ECG findings.

Mutation Analysis. DNA sequencing of exon 7 in the proband (III-1; Fig. 2) identified a heterozygous G-to-C mutation at position 1681. This missense mutation was predicted to change an alanine for a proline (A561P) within the S5 region of HERG. This mutation was also identified in the proband's father and in his elder brother (II-1 and III-2). DNA sequencing of other genes related to LQT (i.e., *KCNQ1*, *KCNE1,* and *SCN5A*) encoding the α- and β-subunits of the I_{Ks} current and the α-subunit of the I_{Na} channel, respectively, did not reveal other mutations.

Clobutinol Blocks HERG Current. We investigated the sensitivity of homomeric WT channels to the nonopioid antitussive clobutinol. Transfected COS-7 cells expressed a large K^+ current, with biophysical properties reminiscent of those of the rapid component of the cardiac delayed-rectifier K^+ current recorded in human cardiac cells (Fig. 3A) (Wang et al., 1994). When repolarized to −70 mV, expressing COS-7 cells exhibited a large deactivating current (I tail). The half-activation potential ($V_{1/2}$) for this current was calculated as −10.4 ± 5 mV (n = 10). Clobutinol at 10^{-5} M induced a slow decay of the activating current recorded at +10 mV suggesting, voltage-dependent block and a lesser blocking effect at the initial phase of activation. This pattern of inhibition was

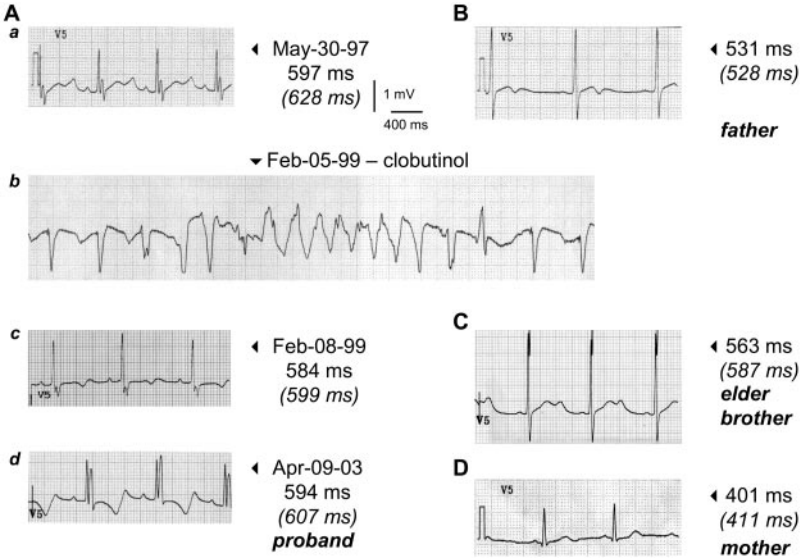

Fig. 1. ECG tracings in lead V5 of the proband (A), his father (B), his eldest brother (C), and his mother (D). Only the mother was not an A561P HERG carrier. QTc_{Bazett} and $QTc_{Fredericia}$ (shown in parentheses in italic type) values are also indicated.

observed at the steady state. After full activation at +10 mV, clobutinol inhibited the HERG tail current with a half-maximum block concentration (IC_{50}) of $2.9 \cdot 10^{-6} \pm 0.7 \cdot 10^{-6}$ M and a Hill coefficient of 0.9 ($n = 9$) (Fig. 3B).

As illustrated in Fig. 3C, the HERG-related K^+ current activated at potentials positive to −50 mV and exhibited strong inward rectification. Deactivating K^+ currents reached a maximum after a prepulse to 10 mV and did not further increase with more positive depolarizing prepulses (Fig. 3D). As depicted in Fig. 3, C and D, clobutinol decreased activating and deactivating currents. The inset in Fig. 3D shows that clobutinol blocked the tail current more effectively at depolarized potentials ($p < 0.001$). Recovery from block was also analyzed when the membrane potential was repolarized to −70 mV. After a depolarization to +10 mV, the initial deactivating current measured at the beginning of the repolarizing pulse (I tail init) was significantly more inhibited than that measured 500 ms later (I tail late) (10^{-5} M clobutinol, 71 ± 5 versus 45 ± 13%; inhibition percentage of I tail init and I tail late, respectively; $n = 7$, $p < 0.05$). We conclude that the HERG block as produced by clobutinol was voltage-dependent inasmuch as it was more pronounced at depolarizing voltages and as it developed with depolarization and relaxed with repolarization.

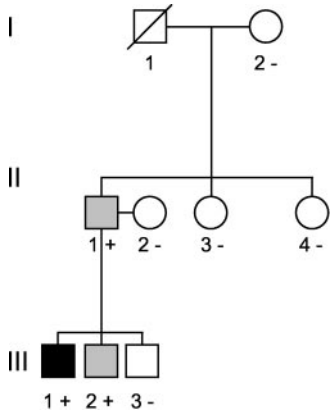

Fig. 2. Pedigree of the family. Empty symbols (circles, female family members; squares, male family members) depict unaffected members, gray symbols depict members presenting a long QTc only, and the black symbol represents the member who experienced torsades de pointes. +, carriers of A561P HERG mutation; −, noncarriers.

Electrophysiological Properties of the HERG A561P, HERG A561T, and HERG A561V Channels. Because the nonopioid antitussive drug clobutinol had triggered arrhythmias in the A561P HERG carrier, we evaluated the effects of this mutation on the channel function. The functional effects of A561P were also compared with those caused by A561T and A561V mutations. In cells injected into the nucleus with either A561P HERG, A561T HERG, or A561V HERG, no current was recorded, unlike in cells injected with WT HERG, suggesting that the three mutations led to a complete loss of function (Fig. 4A). Because patients with LQT are

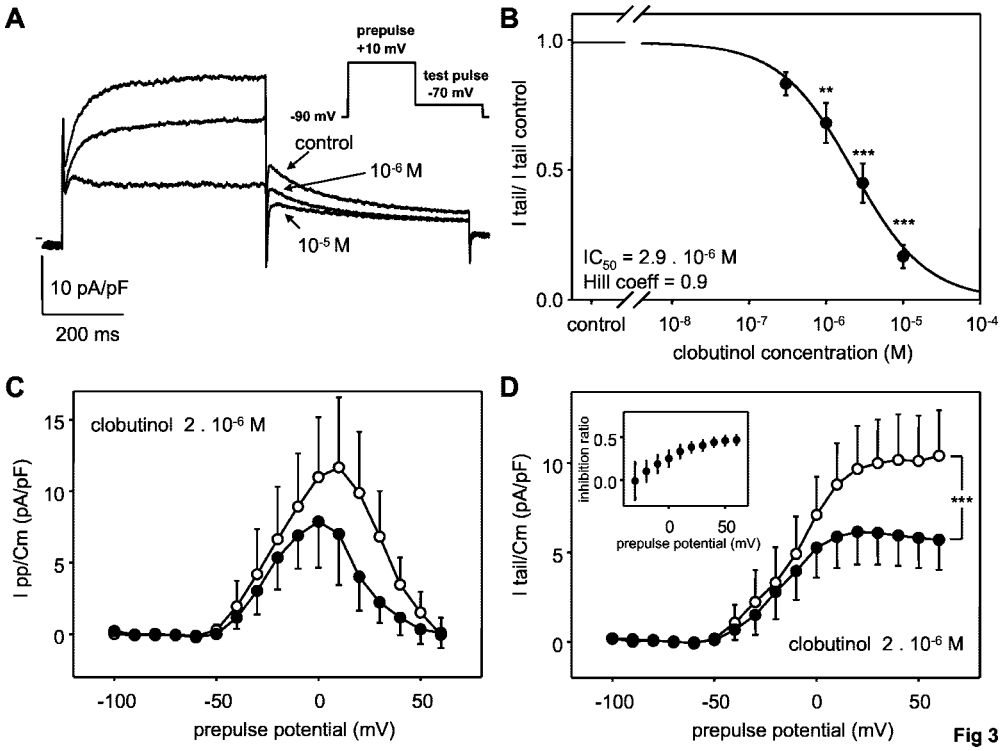

Fig. 3. A, effects of clobutinol on HERG K^+ currents expressed in COS-7 cells. Representative current traces recorded in cells expressing WT HERG in control condition and in the presence of increasing clobutinol concentrations. Voltage protocol (500-ms steps) was as shown in the inset. B, dose-response curve for clobutinol to block the HERG tail current ($n = 9$). Voltage protocol used was the same as that described in A. Tail current was normalized to the control value and expressed as a function of the drug concentration. Solid line, fit of experimental data to the Hill equation $y = a + \{d/[1 + (x/c)^{n_H}]\}$, where x is the drug concentration and n_H is the Hill coefficient. IC_{50} value was calculated as the drug concentration for which y = 50%. ⋆⋆, $p < 0.01$; ⋆⋆⋆, $p < 0.001$. C, current-voltage relation for activated current (prepulse current, I_{pp}) density in control (I_{pp}/C_m; ○) and in the presence of 2.10^{-6} M clobutinol (●; $n = 10$). Voltage protocol consisted of 500-ms depolarizing and hyperpolarizing prepulses to various potentials between −100 and +60 mV followed by a test pulse to −70 mV for 500 ms. Holding potential, −90 mV; frequency, 0.33 Hz. D, current-voltage relation for the deactivating tail current (I_{tail}) density under control conditions (I_{tail}/C_m; ○) and with 2.10^{-6} M clobutinol (●; $n = 10$). ⋆⋆⋆, $p < 0.001$. Inset, inhibition ratio (1 − [I_{tail} in the presence of 2.10^{-6} M clobutinol/I_{tail} control]) versus prepulse potential ($n = 9$–10).

heterozygous for these HERG mutations, mutant and WT proteins were coexpressed with appropriate ratios to mimic the genotype of the mutation carriers. As shown in Fig. 4B, the tail K^+ current density measured at −70 mV (depolarizing test pulse to +10 mV) was markedly reduced to approximately 30% of the control current. We concluded that the three mutations altered the WT HERG channel function in a dominant-negative manner.

The absence of measurable K^+ currents for mutated homomeric channels can be related to either a defect in channel targeting to the plasma membrane or altered gating properties of channels. To test whether homomeric channels are inserted into the cell membrane, immunolocalization experiments were conducted. As illustrated in Fig. 4A, WT HERG-expressing cells showed an intracellular and plasma-membrane staining, whereas membrane staining was undetectable with A561P, A561T, and A561V HERG channels, suggesting that these channels do not insert into the cell membrane. In cells cotransfected with WT and mutant HERG, confocal microscopy revealed that membrane staining was still detectable, although less intensely (Fig. 4B). These results suggest that the mutated channels are poorly processed to the plasma membrane and that heterotetramers coexpressed with the WT protein are mostly retained in intracellular compartments.

In addition to the strong reduction in current amplitude, the A561P mutation also modified the voltage-dependence of activation of the WT + A561P heteromeric channels (Fig. 5, A and B) and produced a significant shift of $V_{1/2}$ toward more negative potentials (Table 1). The small 3- to 3.5-mV shift seen in cells coexpressing WT + A561V or A561T HERG was not significant. On the other hand, the slope factor of activation was slightly but significantly modified, demonstrating

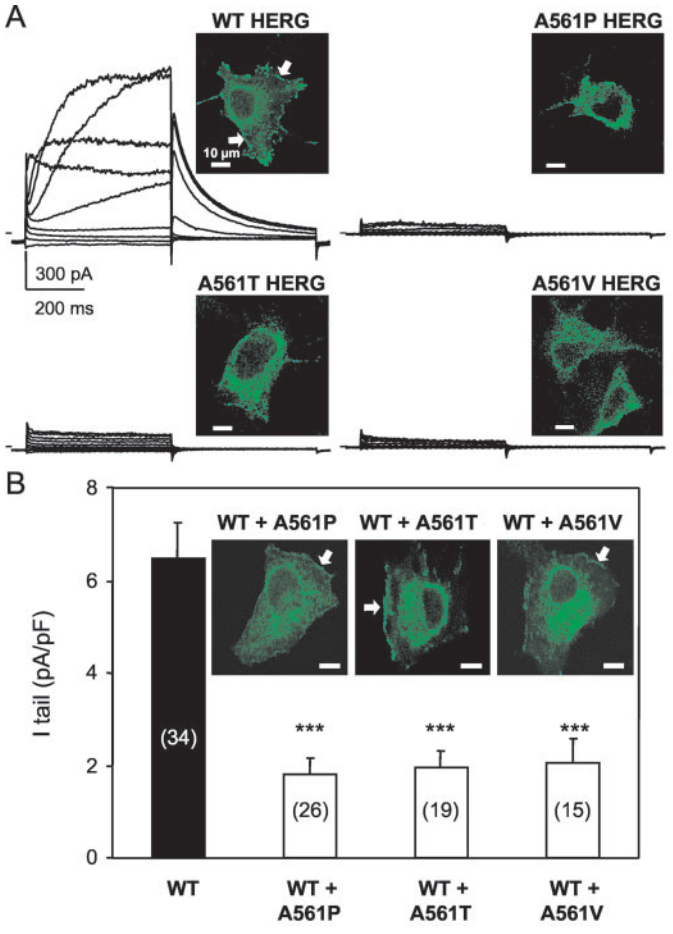

Fig. 4. A, current recorded from WT HERG–, A561P HERG–, A561T HERG–, or A561V HERG–injected COS-7 cells. Voltage protocol used was the same as that described in Fig. 3B. B, tail current density recorded at −70 mV after a depolarization to +10 mV in cells either injected with cDNA coding for WT HERG or coinjected with WT HERG cDNA plus A561P, A561T or A561V HERG cDNA. Statistical significance versus WT: ⋆⋆⋆, $p < 0.001$. Insets, confocal laser scanning images of COS-7 transfected with the different cDNAs. White arrows, membrane staining.

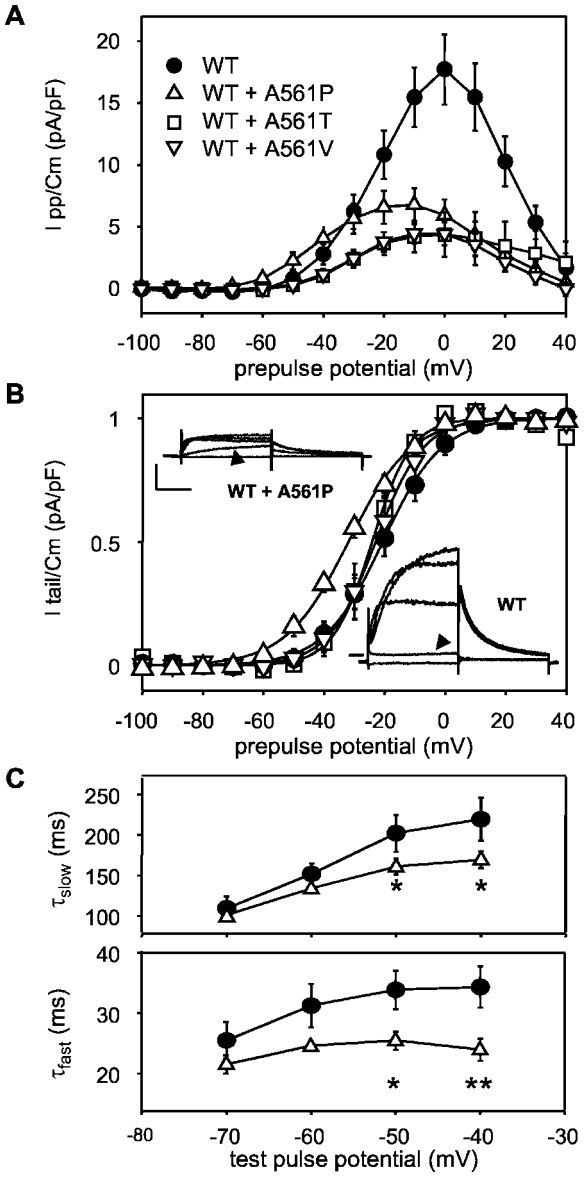

Fig. 5. A, prepulse current density (I_{pp}/C_m) versus potential in cells either injected with WT HERG ($n = 13$) or coinjected with WT HERG plus A561P HERG ($n = 12$), A561T HERG ($n = 9$), or A561V HERG ($n = 9$). The same voltage protocol was used as described in Fig. 3C. B, relative tail current versus prepulse potential. Inset, representative current traces recorded in cells polarized at −100, −40 (black arrows), 0, +20, and + 40 mV (scales: 5 pA/pF and 200 ms) in cells expressing WT HERG or WT + A561P HERG channels. C, the tail current recorded at various potentials after a depolarization to +10 mV was fitted using the equation $I\ (t) = a_f \exp(-t/\tau_f) + a_s \exp(-t/\tau_s)$, where a_f and a_s represent the respective proportion of the fast (τ_f) and slow (τ_s) deactivation processes. τ_f (bottom) and τ_s (top) are plotted as a function of test pulse potential for HERG WT tail currents ($n = 13$) and for WT + A561P HERG tail currents ($n = 7$). Statistical significance versus WT: ⋆⋆, $p < 0.01$; ⋆, $p < 0.05$.

the alteration of the channel gating induced by the mutations.

In cells coexpressing WT + A561P HERG, we also observed a reduction in the fast and slow deactivation time constants when the deactivating current traces were fitted using a double exponential function (Fig. 5C). The fast deactivating component contributed to approximately 40% of the WT or WT + A561P current at any tested potential. Altogether, the modifications as induced by the A561P mutation (i.e., current reduction and faster deactivation kinetics counterbalanced by the shift in the activation curve) should lead to a milder loss of function of the WT + A561P channels compared with the A561V or A561T mutations, which only produced a decrease in current amplitude.

To visualize more accurately the functional effects of the mutants, a human ventricular action potential voltage clamp wave form was applied to cells expressing WT or WT + mutated HERG channels. The normalized currents resulting from this stimulation are depicted in Fig. 6. The HERG current, shown as the E-4031–sensitive current, increased progressively as the action potential repolarized to reach a peak. In accordance with the shift of the activation curve of WT + A561P channels, an earlier WT + A561P HERG current peak was seen during the action potential time course. This behavior should presumably lead to a less pronounced QT interval lengthening in comparison with WT + A561T or WT + A561V channels.

Clobutinol Blocks WT + A561P HERG Current. The effects of clobutinol were further tested in cells coexpressing WT + A561P HERG channels. Figure 7 illustrates that the sensitivity of heteromeric channels to the block produced by clobutinol was similar to that of homomeric channels (IC_{50} for clobutinol on heteromeric WT + A561P HERG, 1.9 $10^{-6}\pm$ 0.7 10^{-6} M; Hill coefficient, 1.1; $n = 5$).

Functional Implications. Electrophysiological data demonstrate that each of the WT + A561P, WT + A561T, and WT + A561V HERG currents is characterized by a decrease in current density to ≈30% of the control WT value. In addition, the WT + A561P HERG current shows alterations in kinetics (i.e., a −11 mV shift in voltage dependence) of activation as well as a ≈30% decrease in fast and slow time constants of deactivation. To assess the functional consequences of these alterations, we carried out computer simulations using the comprehensive human ventricular cell model by Priebe and Beuckelmann (1998). Figure 8A (top) shows the model action potential with normal I_{Kr} (broken line) and with a 70% reduction in I_{Kr} (solid line), representing the experimentally observed reduction in HERG current density. The reduction in repolarizing current induces a prolongation of the action potential by 124 ms (arrow). The experimentally observed alterations in kinetics result in an earlier activation of HERG channels and thus in a larger I_{Kr} amplitude (Fig. 8B). Despite the more rapid deactivation of the current, repolarization is accelerated and the action potential shortened by 33 ms. When combined, the two effects (i.e., the reduction in current density and alterations in kinetics) are almost additive, with an AP prolongation of 97 ms (Fig. 8C). We also tested the effects of the experimentally observed

TABLE 1

Activation parameters of WT, WT + A561P, WT + A561T, and WT + A561V HERG currents

Voltage protocol was the same as described in Fig 3C. Tail currents were fitted using a Boltzmann equation: $I_{tail}/I_{tail\ max} = 1/\{1 + \exp[-(V_{pp} - V_{1/2})/k]\}$, where $I_{tail\ max}$ is peak I_{tail}, V_{pp} is the prepulse potential, $V_{1/2}$ is the prepulse voltage for which I_{tail} is half of $I_{tail\ max}$, and k is the slope factor. WT was tested versus data obtained when PEI was used as transfection vector (see clobutinol experiments) and WT + A561s versus WT.

	$V_{1/2}$	k	n
	mV		
WT	−20.7 ± 3.0*	8.0 ± 0.4*	13
WT + A561P	−31.8 ± 2.1**	10.0 ± 0.6**	12
WT + A561T	−24.2 ± 2.1*	6.0 ± 0.4**	9
WT + A561V	−23.5 ± 3.6*	6.2 ± 0.3**	9

*, not significant; **, $p < 0.01$.

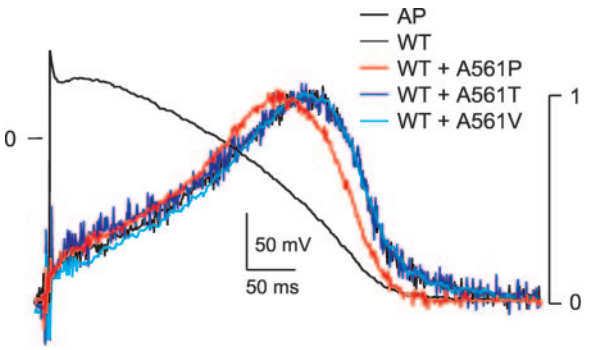

Fig. 6. Respective contribution of HERG current during a cardiac action potential. An action potential wave form recorded from a human ventricular myocyte was used as the command voltage to clamp HERG-transfected COS-7 cells. HERG currents are expressed as the normalized E-4031–sensitive current (control current − residual current in 300 nM E-4031).

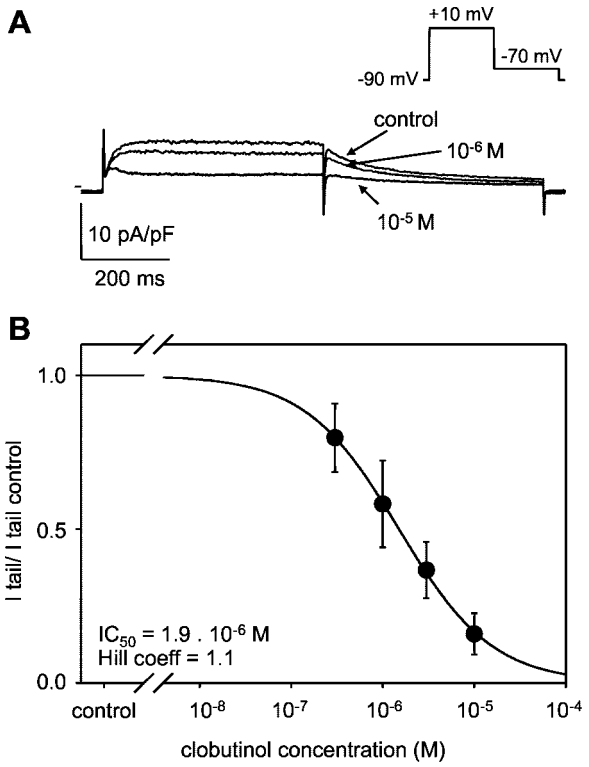

Fig. 7. Effects of clobutinol on WT + A561P HERG K^+ currents expressed in COS-7 cells. A, representative current traces recorded in cells expressing WT + A561P HERG in control condition and in the presence of growing clobutinol concentrations. Voltage protocol used was as described in Fig. 3A. B, dose-response curve for WT + A561P HERG K^+ tail current ($n = 4$). Normalization and fitting was done as described in Fig. 3B.

changes in slope of the HERG channel-activation curve (Table 1), but the effects thereof were very small, with a change in APD_{90} (ΔAPD_{90}) typically less than 1 to 2 ms (data not shown). We also determined ΔAPD_{90} for pacing cycle lengths other than 1 s (Fig. 8D). In all cases, the effects are more pronounced at shorter cycle lengths (i.e., at higher heart rate), which was also observed in a canine AP model for other mutations that affect I_{Kr} (Mazhari et al., 2001). Figure 8D also shows that the A561P HERG mutation (△) exerts milder effects than the A561T or A561V mutations (□). However, application of clobutinol (simulated by a 30% block of I_{Kr}, in accordance with the estimated circulating drug concentration of 0.55 to 0.75 μM and the dose-response curve shown in Fig. 7) (Zimmer et al., 1977) increases AP prolongation for the A561P mutation to values greater than those for the more severe A561T or A561V mutations (Fig. 8D, ▲). With wild-type HERG channels, clobutinol per se produces a mild prolongation of the action potential at all pacing cycle lengths (Fig. 8D, ●).

Increased dispersion of repolarization across the ventricular wall, either arising from dynamic factors (steeper APD restitution) or from enhanced heterogeneity in intrinsic electrophysiological properties among different cell types, is an important determinant of the susceptibility to ventricular arrhythmias (Qu et al., 2000). Therefore, we first tested whether the HERG channel mutations would steepen the APD restitution curve (Fig. 8E). Again, the largest effects are observed for the A561T or A561V mutations. However, application of clobutinol significantly steepens the APD restitution curve for the A561P mutation, yielding a slope near 1 for the steepest part of the curve. With wild-type HERG channels, clobutinol produces only moderate alteration in the restitution curve. Next, we assessed the effects of the HERG channel mutations on the intrinsic differences among the different cell types. Figure 8F shows that the mutations preferentially prolong the M cell action potential, thereby increasing the dispersion of repolarization. The largest dispersion is obtained for the WT + A561P HERG current in the presence of clobutinol (189 ms versus a control value of 59 ms).

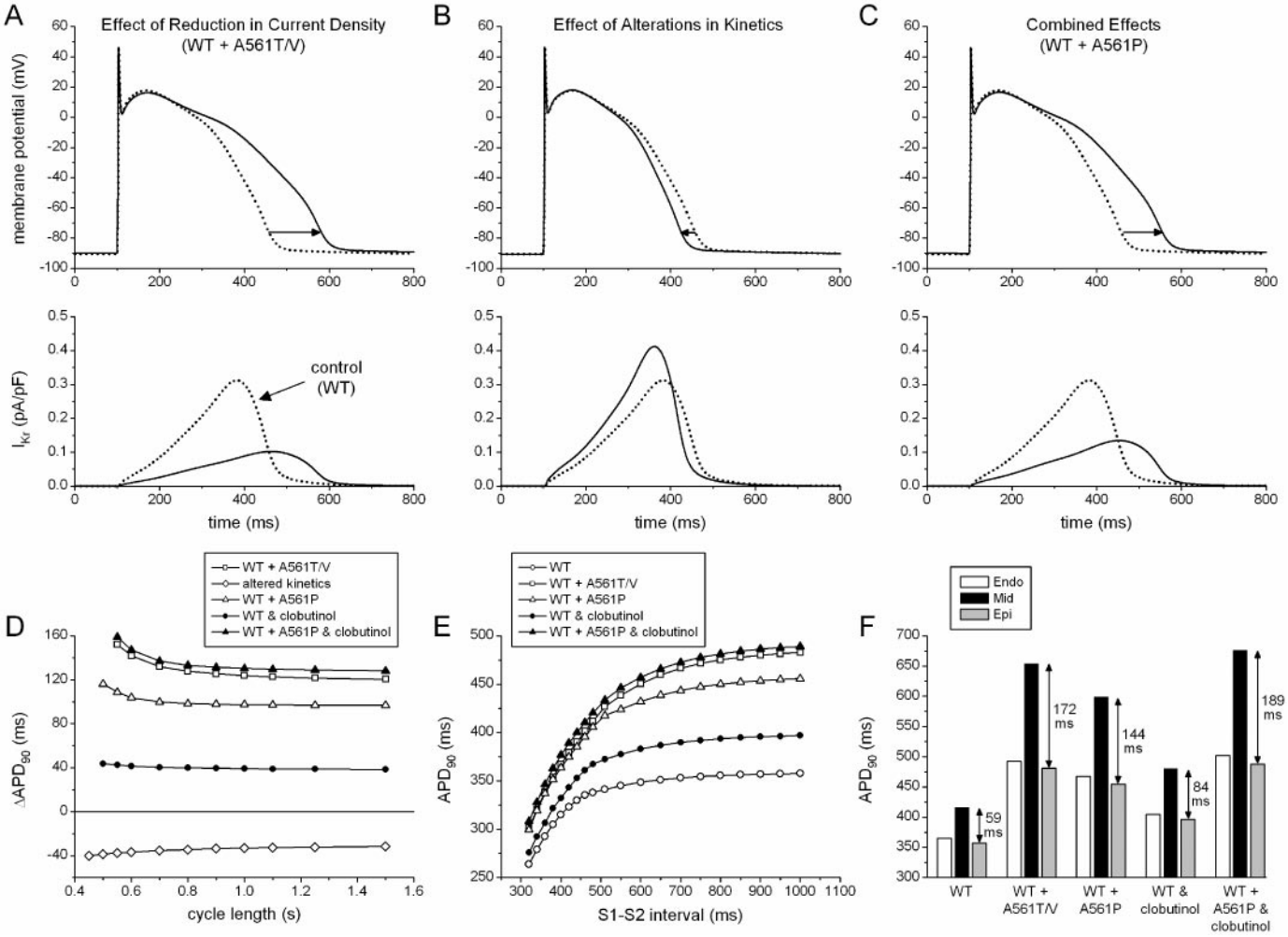

Fig. 8. The A561P HERG channel mutation exerts smaller effects on the cardiac action potential than the A561V or A561T mutation, but not if the WT + A561P HERG current is partially blocked by clobutinol. A–C, Action potentials elicited at 1 Hz (top) and associated I_{Kr} (bottom) in the case of a 70% decrease in HERG current density, as observed for all three mutations (A); alterations in HERG current kinetics as observed for the A561P mutation (i.e., a −11 mV shift in voltage dependence of activation as well as a ≈30% decrease in fast and slow time constants of deactivation) (B); and both changes (C). Broken lines indicate WT control. D, change in APD_{90} (ΔAPD_{90}) at various pacing cycle lengths. E, APD restitution curves for each of the HERG channel mutations. F, effects of the HERG channel mutations on differences in APD_{90} of endocardial, midmyocardial, and epicardial cells upon 1-Hz stimulation.

It has been hypothesized that the AP prolongation associated with LQT favors the development of early after-depolarizations (EADs) and triggered activity caused by reactivation of the L-type calcium current ($I_{Ca,L}$) during the AP plateau. In contrast with simulation studies using the Luo-Rudy guinea pig-type AP model (Viswanathan and Rudy, 1999), we did not observe EADs in any of the three cell types studied. As discussed by Priebe and Beuckelmann (1998), the lower susceptibility of their human ventricular cell model to the generation of EADs could reflect an inherent property of human tissue. We did, however, observe considerably delayed repolarization for the M cell model in the case of the A561 HERG channel mutations, especially in response to moderate increases in $I_{Ca,L}$, with APD_{90} values exceeding 1 s upon a 25% increase in $I_{Ca,L}$ (data not shown).

In summary, Fig. 8 shows that the effects of the A561P mutation on basic AP properties are constantly less severe than those of the A561V or A561T mutation but become more severe if the WT + A561P HERG current is further reduced by the application of clobutinol.

Discussion

This report is the first to detail the effects of clobutinol, a commonly used antitussive drug, on the HERG cardiac K^+ channel. The rhythmic incident correlated to clobutinol intake in the proband revealed the potential effects of the drug and instigated the present study, which also resulted in the identification of a novel HERG mutation responsible for LQT2.

Drug-Induced Action Potential Prolongation. We found that clobutinol displays an IC_{50} of $\approx 2\ \mu M$ on HERG. As illustrated by computer modeling, clobutinol would induce only mild modifications in the ventricular action potential duration of unaffected individuals. The effects of clobutinol displayed a positive voltage dependence, suggesting that the molecule interacts with an activated state of the HERG channel. Drugs that block HERG current, are often associated with QT prolongation and development of the ventricular arrhythmia known as torsades de pointes. Among them are terfenadine, astemizole, and cisapride. Published IC_{50} values ranged between 56 and 431 nM for terfenadine (Rampe et al., 1997; Chachin et al., 1999) and between 69 and 480 nM for astemizole (Taglialatela et al., 1998; Chachin et al., 1999). Cisapride IC_{50} values ranged between 4.3 nM in human embryonic kidney 293 cells (Anson et al., 2004) and 124 nM in *Xenopus laevis* oocytes (Fernandez et al., 2004). We investigated previously the effects of cisapride and measured an IC_{50} value of 240 nM (Potet et al., 2001). We and others (Walker et al., 1999) have shown that the inhibition produced by cisapride increases during depolarization and is partially removed during repolarization. In our previous and present works, the cells were depolarized for 500 ms only, a duration close to the human action potential duration but much shorter than the duration used by previous investigators (2- to 20-s duration prepulses). Because cisapride produces a time-dependent open-channel block, the affinity of cisapride for HERG may be overestimated when long depolarization duration protocols are used. Because clobutinol is also a voltage-dependent blocker, it is more accurate to compare clobutinol and cisapride IC_{50} values for relatively brief depolarizations. Under these conditions, clobutinol has an IC_{50} value that is approximately 10 times higher than that of terfenadine, astemizole, or cisapride. This may explain why clobutinol, despite widespread clinical use in Europe, has not yet been reported to produce QT prolongation. On the other hand, the long QT syndrome may often be missed in patients presenting syncope, seizures, or drop attacks (Pacia et al., 1994). This may hold for a previously reported case of grand mal seizure associated with clobutinol overdose (Ramirez et al., 1993). In conclusion, the absence of other case reports involving clobutinol and its relatively high IC_{50} value exclude this drug from the list of drugs with risk of torsades de pointes, although the potential inhibitory activity of clobutinol may represent an aggravating factor when the cardiac repolarization reserve is already reduced, as in patients with congenital LQT like the proband in the present study.

Trafficking of Mutant HERG Proteins. Among the mechanisms underlying LQT2, impaired trafficking of HERG protein is increasingly recognized as a leading cause. In vitro, the A561P mutation caused defects in intracellular protein transport to the plasma membrane. Furthermore, the mutant subunit coexpression reduced the WT HERG function by a dominant-negative effect. Similar results were obtained with A561V or A561T HERG, two LQT2 mutations that were identified previously (Curran et al., 1995; Dausse et al., 1996). Studying the A561V dominant-negative mechanism, Ficker et al. (2000) observed that coassembly of WT with A561V HERG prevented the traffic of the heteromeric channels to the plasma membrane. Our results are in favor of a similar mechanism concerning A561T or A561P HERG mutants. Numerous HERG mutations leading to trafficking deficiency have been described throughout the protein (Paulussen et al., 2002). Key regions of the protein for trafficking have been described in the C-terminal part of the protein as well as in the N-terminal–located PAS domain (Kupershmidt et al., 2002; Paulussen et al., 2002; Akhavan et al., 2003). Retention of mutant proteins has also been associated with increased affinity with the chaperones heat shock protein 70 and heat shock protein 90 (Ficker et al., 2003). However the amino acids involved in this association are localized in the S5–p-loop linker or in the C-terminal tail, unlike the Ala561.

HERG Channel Mutations at Position 561. Assuming random coassembly of WT and mutant HERG subunits and also that only WT homotetramers are conductive, the K^+ current resulting from heterozygous expression should be reduced to $1/16^{th}$ of the WT current value. Subsistence of a current $>1/16^{th}$ of WT K^+ current indicates that the association of WT and mutated HERG is less frequent than homomeric association or, alternatively, that some heteromeric channels can reach the plasma membrane and effectively conduct K^+ current. Concerning the A561P mutation, modifications of the heteromeric K^+ current characteristics (i.e., ≈ -11-mV shift of the activation $V_{1/2}$ and change in deactivation kinetics) are in favor of the second hypothesis. Investigating the effects of A561V HERG mutant, Kagan et al. (2000) suspected a small fraction of current being passed by heteromeric channels. These authors also observed a shift of the activation $V_{1/2}$ in Chinese hamster ovary cells from +0.7 mV in WT HERG-expressing cells to −10.9 mV in WT + A561V HERG-expressing cells. We failed to observe such a ≈ -10-mV shift in COS-7 cells. It has to be mentioned, however, that the study by Kagan et al. was performed at room temperature, unlike ours (35°C). Studying WT HERG bio-

physical properties in human embryonic kidney 293 cells at various temperatures, Zhou et al. (1998) calculated a shift of $V_{1/2}$ value from −14.2 mV at 23°C to −25.9 mV at 35°C. The latter value is close to that of −21.5 mV obtained at the same temperature by Sanguinetti and Jurkiewicz (1990) for the native I_{Kr} in guinea pig ventricular myocytes and to −20.7 mV as in the present study. Because no shift caused by coexpression of WT and A561V HERG proteins could be detected at +35°C, one can suspect that the mutation alters the temperature sensitivity of the heteromeric channel activation. On the other hand, this discrepancy may be explained by the cell model difference (Chinese hamster ovary versus COS-7 cells).

Substitution of the alanine to a valine or a threonine at position 561 seems to have no effect on heteromeric channel activity. On the other hand, the substitution to a proline that may induce a kink in the S5 helix altered its activation and deactivation. By analogy to the Shaker channel structural model, Ala561 is the homolog of Shaker Val414 and faces the S1–S4 voltage sensor (Neale et al., 2003; Torres et al., 2003). Mutations of amino acids facing the voltage-sensor may impair the intersubunit interactions and the coupling of the voltage-sensing function to the channel opening. In addition, S5 structure modification may also alter the pore stability. Finally, because the S4–S5 linker of HERG is involved in the voltage-dependence and kinetics of channel activation and deactivation, it can be suggested that mutations in the S5 helix may be the origin of the heteromeric channel behavior changes by simple allosteric changes, with repercussions on S4–S5 function. However, the activation modifications counterbalance the impaired trafficking consequences and overall lead to milder mutation effects.

Novel LQT2 Mutation. The penetrance of a mutation can be quite variable depending on the family but also among carriers in the same family, as reported for the A561V substitution (Priori et al., 1999). In A561P gene carriers, the only symptom was the lengthening of the QT interval until the proband experienced the drug-induced torsades de pointes. As illustrated in the model simulation provided here, reduction of the resulting K^+ current induces the AP lengthening responsible for the QT interval prolongation. Unlike the other Ala561 substitutions, the A561P mutation induced a more premature I_{Kr} current that, despite its smaller amplitude, limits the AP duration prolongation. This difference from A561V or threonine mutation could, at least in part, explain the milder phenotype of A561P carriers.

Proarrhythmic Effect of Clobutinol. Because the torsades de pointes episode was independent of serum potassium, the drug may be supposed to be the direct trigger of the arrhythmia. Clobutinol has a renal elimination and no known metabolite (Zimmer et al., 1977). The normal kidney function of the proband rules out a possible accumulation of the drug. As illustrated by the computer simulation, clobutinol has only a minor effect on the WT AP duration. Nevertheless, additive moderate reductions of I_{Kr}, first by the HERG A561P mutation and then by clobutinol, may enhance heterogeneity in intrinsic electrophysiological properties among different ventricular cell types, an important determinant of the susceptibility to ventricular arrhythmias. Finally, our work shows that less severe mutation carriers are still at risk of developing arrhythmias when exposed to additional proarrhythmic drug or pathophysiological triggers. It emphasizes the necessity of information on risk factors such as the QT Drug List provided by the University of Arizona Center for Education and Research on Therapeutics resuming the proarrhythmic drugs (http://www.qtdrugs.org/). The reported accident does not necessarily classify clobutinol in list 1 as a "drug with risk of torsades de pointes" but rather in list 3 listing "drugs to be avoided by congenital long QT patients".

Acknowledgments

We thank Estelle Roy, Béatrice Leray, and Marie-Jo Louérat for expert technical assistance.

References

Akhavan A, Atanasiu R, and Shrier A (2003) Identification of a COOH-terminal segment involved in maturation and stability of human ether-a-go-go–related gene potassium channels. *J Biol Chem* **278:**40105–40112.

Anson BD, Ackerman MJ, Tester DJ, Will ML, Delisle BP, Anderson CL, and January CT (2004) Molecular and functional characterization of common polymorphisms in HERG (KCNH2) potassium channels. *Am J Physiol* **286:**H2434–H2441.

Chachin M, Katayama Y, Yamada M, Horio Y, Ohmura T, Kitagawa H, Uchida S, and Kurachi Y (1999) Epinastine, a nonsedating histamine H1 receptor antagonist, has a negligible effect on HERG channel. *Eur J Pharmacol* **374:**457–460.

Conrath CE, Wilders R, Coronel R, de Bakker JMT, Taggart P, de Groot JR, and Opthof T (2004) Intercellular coupling through gap junctions masks M cells in the human heart. *Cardiovasc Res* **62:**407–414.

Curran ME, Splawski I, Timothy KW, Vincent GM, Green ED, and Keating MT (1995) A molecular basis for cardiac arrhythmia: HERG mutations cause long QT syndrome. *Cell* **80:**795–803.

Dausse E, Berthet M, Denjoy I, André-Fouet X, Cruaud C, Bennaceur M, Fauré S, Coumel P, Schwartz K, and Guicheney P (1996) A mutation in HERG associated with notched T waves in long QT syndrome. *J Mol Cell Cardiol* **28:**1609–1615.

Fernandez D, Ghanta A, Kauffman GW, and Sanguinetti MC (2004) Physicochemical features of the HERG channel drug binding site. *J Biol Chem* **279:**10120–10127.

Ficker E, Dennis AT, Obejero-Paz CA, Castaldo P, Taglialatela M, and Brown AM (2000) Retention in the endoplasmic reticulum as a mechanism of dominant-negative current suppression in human long QT syndrome. *J Mol Cell Cardiol* **32:**2327–2337.

Ficker E, Dennis AT, Wang L, and Brown AM (2003) Role of the cytosolic chaperones Hsp70 and Hsp90 in maturation of the cardiac potassium channel HERG. *Circ Res* **92:**e87–e100.

Kagan A, Yu Z, Fishman GI, and McDonald TV (2000) The dominant negative LQT2 mutation A561V reduces wild-type HERG expression. *J Biol Chem* **275:**11241–11248.

Keating MT (1995) Genetic approaches to cardiovascular disease. Supravalvular aortic stenosis, Williams syndrome and long-QT syndrome. *Circulation* **94:**142–147.

Kupershmidt S, Yang T, Chanthaphaychith S, Wang Z, Towbin JA, and Roden DM (2002) Defective human ether-a-go-go-related gene trafficking linked to an endoplasmic reticulum retention signal in the C terminus. *J Biol Chem* **277:**27442–27448.

Liu DW and Antzelevitch C (1995) Characteristics of the delayed rectifier current (I_{Kr} and I_{Ks}) in canine ventricular epicardial, midmyocardial and endocardial myocytes. A weaker I_{Ks} contributes to the longer action potential of the M cell. *Circ Res* **76:**351–365.

Liu DW, Gintant GA, and Antzelevitch C (1993) Ionic bases for electrophysiological distinctions among epicardial, midmyocardial and endocardial myocytes from the free wall of the canine left ventricle. *Circ Res* **72:**671–687.

Mazhari R, Greenstein JL, Winslow RL, Marban E, and Nuss HB (2001) Molecular interactions between two long-QT syndrome gene products, HERG and KCNE2, rationalized by in vitro and in silico analysis. *Circ Res* **89:**33–38.

Mohammad-Panah R, Demolombe S, Riochet D, Leblais V, Loussouarn G, Pollard H, Baró I, and Escande D (1998) Hyperexpression of recombinant CFTR in heterologous cells alters its physiological properties. *Am J Physiol* **274:**C310–C318.

Näbauer M, Beuckelmann DJ, Überfuhr P, and Steinbeck G (1996) Regional differences in current density and rate-dependent properties of the transient outward current in subepicardial and subendocardial myocytes of human left ventricle. *Circulation* **93:**168–177.

Neale EJ, Elliott DJ, Hunter M, and Sivaprasadarao A (2003) Evidence for intersubunit interactions between S4 and S5 transmembrane segments of the Shaker potassium channel. *J Biol Chem* **278:**29079–29085.

Pacia SV, Devinsky O, Luciano DJ, and Vazquez B (1994) The prolonged QT syndrome presenting as epilepsy: a report of two cases and literature review. *Neurology* **44:**1408–1410.

Paulussen A, Raes A, Matthijs G, Snyders DJ, Cohen N, and Aerssens J (2002) A novel mutation (T65P) in the PAS domain of the human potassium channel HERG results in the long QT syndrome by trafficking deficiency. *J Biol Chem* **277:**48610–48616.

Pollard H, Remy JS, Loussouarn G, Demolombe S, Behr JP, and Escande D (1998) Polyethylenimine but not cationic lipids promotes transgene delivery to the nucleus in mammalian cells. *J Biol Chem* **273:**7507–7511.

Potet F, Bouyssou T, Escande D, and Baró I (2001) Gastrointestinal prokinetic drugs have different affinity for the human cardiac human ether-a-go-go K^+ channel. *J Pharmacol Exp Ther* **299:**1007–1012.

Priebe L and Beuckelmann DJ (1998) Simulation study of cellular electric properties in heart failure. *Circ Res* **82:**1206–1223.
Priori SG, Napolitano C, and Schwartz PJ (1999) Low penetrance in the long-QT syndrome: clinical impact. *Circulation* **99:**529–533.
Qu Z, Garfinkel A, Chen PS, and Weiss JN (2000) Mechanisms of discordant alternans and induction of reentry in simulated cardiac tissue. *Circulation* **102:**1664–1670.
Qu Z, Weiss JN, and Garfinkel A (1999) Cardiac electrical restitution properties and stability of reentrant spiral waves: a simulation study. *Am J Physiol* **276:**H269–H283.
Ramirez MS, Rojas AM, Perez LA, Arias IA, Calles M, and Aranguren A (1993) Grand mal seizure and clobutinol overdose. *Vet Hum Toxicol* **35:**444.
Rampe D, Roy ML, Dennis A, and Brown AM (1997) A mechanism for the proarrhythmic effects of cisapride (Propulsid): high affinity blockade of the human cardiac potassium channel HERG. *FEBS Lett* **417:**28–32.
Roden DM, Lazzara R, Rosen M, Schwartz PJ, Towbin J, and Vincent GM (1996) Multiple mechanisms in the long-QT syndrome. Current knowledge, gaps and future directions. The SADS Foundation Task Force on LQTS. *Circulation* **94:**1996–2012.
Sanguinetti MC, Curran ME, Spector PS, and Keating MT (1996) Spectrum of HERG channel dysfunction in an inherited cardiac arrhythmia. *Proc Natl Acad Sci USA* **93:**2208–2212.
Sanguinetti MC, Jiang C, Curran ME, and Keating MT (1995) A mechanistic link between an inherited and an acquired cardiac arrhythmia: HERG encodes the I_{kr} potassium channel. *Cell* **81:**299–307.
Sanguinetti MC and Jurkiewicz NK (1990) Two components of delayed rectifier K^+ current. *J Gen Physiol* **96:**195–215.
Splawski I, Shen J, Timothy KW, Vincent GM, Lehmann MH, and Keating MT (1998) Genomic structure of three long QT syndrome genes: KVLQT1, HERG and KCNE1. *Genomics* **51:**86–97.
Taglialatela M, Pannaccione A, Castaldo P, Giorgio G, Zhou Z, January CT, Genovese A, Marone G, and Annunziato L (1998) Molecular basis for the lack of HERG K^+ channel block-related cardiotoxicity by the H1 receptor blocker cetirizine compared with other second-generation antihistamines. *Mol Pharmacol* **54:**113–121.
Torres AM, Bansal PS, Sunde M, Clarke CE, Bursill JA, Smith DJ, Bauskin A, Breit SN, Campbell TJ, Alewood PF, et al. (2003) Structure of the HERG K^+ channel S5P extracellular linker: role of an amphipathic α-helix in C-type inactivation. *J Biol Chem* **278:**42136–42148.
Viswanathan PC and Rudy Y (1999) Pause induced early after depolarizations in the long QT syndrome: a simulation study. *Cardiovasc Res* **42:**530–542.
Walker BD, Singleton CB, Bursill JA, Wyse KR, Valenzuela SM, Qiu MR, Breit SN, and Campbell TJ (1999) Inhibition of the human ether-a-go-go-related gene (HERG) potassium channel by cisapride: affinity for open and inactivated states. *Br J Pharmacol* **128:**444–450.
Wang Q, Shen J, Splawski I, Atkinson D, Li Z, Robinson JL, Moss AJ, Towbin JA, and Keating MT (1995) SCN5A mutations associated with an inherited cardiac arrhythmia, long QT syndrome. *Cell* **80:**805–811.
Wang Z, Fermini B, and Nattel S (1994) Rapid and slow components of delayed rectifier current in human atrial myocytes. *Cardiovasc Res* **28:**1540–1546.
Zhou Z, Gong Q, Ye B, Fan Z, Makielski JC, Robertson GA, and January CT (1998) Properties of HERG channels stably expressed in HEK 293 cells studied at physiological temperature. *Biophys J* **74:**230–241.
Zimmer A, Buecheler A, and Kaschke S (1977) Pharmacokinetic comparison of clobutinol HCl (with and without orciprenaline SO_4) as solution, liquid and syrup in man. *Arzneimittelforschung* **27:**2011–2017.

Address correspondence to: Dr. Isabelle Baró, INSERM U533, Faculté de Médecine, 1, rue Gaston Veil, 44035 Nantes, France. E-mail: isabelle.baro@nantes.inserm.fr